

# Oral Formulation of Posaconazole in Nanosuspension: Development and Optimization by Design of Experiments Approach

T. V. Gautham<sup>1</sup>, Rakesh Patel<sup>1</sup>, V. Rama Mohan Gupta<sup>2</sup>, G. Parimala Devi<sup>3</sup>,  
Abhay Dharamsi<sup>1</sup>

<sup>1</sup>Department of Pharmaceutics, Parul University, Vadodara, Gujarat, India, <sup>2</sup>Department of Pharmaceutics, Pulla Reddy Institute of Pharmacy, Hyderabad, Telangana, India, <sup>3</sup>Department of Pharmacognosy, Pulla Reddy Institute of Pharmacy, Hyderabad, Telangana, India

## Abstract

**Introduction:** FR and D scientists continuously try to increase the *in vivo* performance of low soluble and poor bioavailable drugs using various formulation techniques. Nanosuspensions are relatively simple to develop and fall within the novel drug delivery approaches. **Materials and Methods:** The polymers such as soya lecithin, Tween 80, poloxamer, and polyethylene glycol were used for the preparation. Central composite design was used to optimize the posaconazole nanosuspension and formulation was characterized for various parameters, that is, particle size, morphology and physicochemical parameters were evaluated for *in vitro* and *in vivo* performance. **Results:** Optimized nanosuspension contained an average particle size of  $219 \pm 0.25$  nm and zeta potential was  $-19.3 \pm 6.73$  mV. The optimized nanosuspension displayed a significant increase in dissolution profile, by more than 4 folds on average as compared to the drug within 60 min. The results of the pharmacokinetic (PK) study showed the optimized nanosuspension releases the drug with maximum bioavailability as compared to marketed formulation. The formulation found stable up to 6 months. **Conclusion:** The development of nanosuspension resulted in superior performance in PK effects over the marketed formulation.

**Key words:** Central composite design, *in vitro* drug release, nanosuspension, pharmacokinetics, posaconazole

## INTRODUCTION

Regardless of the route of administration, solubility is a critical component of the drug for determining its effectiveness. It also poses a major challenge for pharmaceutical companies developing new pharmaceutical products, as nearly half the active substances are either insoluble or poorly soluble in water. To reduce these difficulties, various formulation approaches were developed involving the use of surfactants, cosurfactants, lipids/oils, permeation enhancers, cosolvents, cyclodextrines, and techniques such as micronization, salt formation, and nanoparticles. At present, much focus is given to nano-based drug delivery systems, which improve the oral BA of BCS class II drugs. The absorption of drugs from delivery systems depends on factors like, that is, particle size and rate of dispersion of drugs.<sup>[1,2]</sup>

Nanosuspensions (NPs) are a colloidal dispersion of particles that are nanosized and stabilized with

the help of surfactants. Nanosuspensions are also defined as the biphasic system, which consists of drug particles that are dispersed in aqueous vehicles with a diameter of less than a mean particle size of 200–600 nm. NPs can be used either for topical, or oral use or for pulmonary and parenteral administration with lowered particle size, resulting in an increased dissolution rate and thus enhanced bioavailability.<sup>[3,4]</sup>

Nanosuspensions are a unique and provide solution to the issues associated with hydrophobic drugs, such as low solubility and poor bioavailability. For large-scale production of NPs, milling and high-pressure homogenization technologies have

### Address for correspondence:

T. V. Gautham, Department of Pharmaceutics, Parul Institute of Pharmacy, Vadodara, Gujarat, India.  
Phone: 008008555414.  
E-mail: gautham.talla@gmail.com

**Received:** 23-01-2023

**Revised:** 21-04-2023

**Accepted:** 08-05-2023

been successfully used. The physicochemical characteristic properties such as improvement of dissolution velocity, increased saturation solubility, improved bioadhesivity, versatility in surface modification, and ease of postproduction processing, have widened the applications of NPs for various routes of administration. The applications of NPs in oral and parental routes have been very well established, although applications in pulmonary and ocular delivery have to be evaluated. However, their delivery through buccal, nasal, and topical delivery is yet to be performed.

The broad class of formulation excipients contained in nanosuspensions may affect the performance of a dosage form. Various QBD techniques such as the application of response surface methodology (RSM) employing fractional factorial designs/full factorial designs such as Box–Behnken and central composite design (CCD) are used for preparing an optimized formulation.<sup>[5,6]</sup> This study is important as it determines the effect of variables on responses, determination of process, and parameters' interactions. The major advantage of RSM is to reduce the number of trial runs in optimizing the formulation contributing to reductions in time and cost. Among different RSMs, CCD is a popular form to understand the interactions among the parameters and responses that are optimized.<sup>[7]</sup>

The aim of our research was to apply experimental design methodology in the development and optimization of posaconazole nanosuspension. Posaconazole is a hydrophobic drug so it was selected for nanosuspension formulation. CCD, a three-level three-factorial design, was used to characterize and optimize the formulation and finally evaluated for *in vitro* and *in vivo* performance.

The objective of the present work was to develop optimal nanosuspension of posaconazole by CCD to improve oral bioavailability.

## MATERIALS AND INSTRUMENTS

The posaconazole drug was procured as a gift sample from Strides Shashun, Bangalore. The other excipients such as Tween 80 (monohydrate GR), Soya lecithin, Poloxamer 188, and PEG 6000 were sourced from Merck Limited, Mumbai, India. Electronic Balance (Contech Electronic Balance), High-Speed Homogenizer – Model Panda PLUS 2000, UV-VIS Spectrophotometer, Model JASCOV-530-Spectra Lab, Zetasizer Nano S90 Particle Size Analyzer, Malvern Instruments, Malvern, UK, Zetasizer 300 HAS, and Malvern Instruments, Malvern, UK were used in the development and optimization of posaconazole nanosuspension.

### Methods

#### Formulation of nanosuspension

Nanosuspension was formulated using a high-pressure homogenizer (HPH) (Panda PLUS 2000, GEA Niro Soavi,

Germany). To prevent blocking of the homogenizer valve, the coarse powder of drugs was first dispersed in an aqueous stabilizer solution using a digital homogenizer at 8000 rpm for 1 h to form primary nanosuspension. The primary nanosuspension was further processed through a HPH with three homogenization cycles at 250, 700, and 1200 bars, followed by maximum cycles at 1500 bars. By varying the number of cycles of homogenization and keeping, the process temperature constant at 25°C different particle sizes of nanosuspension was obtained.<sup>[4,8]</sup>

### Application of CCD

The CCD of the RSM using a five-level full factorial study was performed to explore the optimum levels of the variables after following Plackett–Burman screening design and identifying critical process variables. This methodology consists of two groups of design points, which include two-level factorial design points (–1 and +1) and axial or star points (– $\alpha$  and + $\alpha$ ) along with center points (0). Three selected independent variables that have the highest percentage contribution were selected from Packet Berman (PB) design and further studied at five different levels coded as – $\alpha$ , –1, 0, +1, and + $\alpha$  using CCD. The value for  $\alpha$  (1.6817) was calculated to fulfill the design rotatability. Response variables selected are particle size (Y1), drug content (Y2), and entrapment efficiency (Y3). The CCD matrix was designed using Design Expert® software (Version 11.0.5.0, Stat-Ease Inc., MN), with 20 runs, including one replication of a fractional point, one axial point, and six replicated center points. According to the obtained CCD matrix, the 20 nanosuspension formulations were prepared and evaluated for responses to proceed with model fitting. The data are shown in Table 1. For the current optimization study, different RSM computations were performed and polynomial equations that contain quadratic and interaction terms were produced for all the dependent factors.<sup>[9]</sup>

### Saturation solubility studies

Saturation solubility was done with the addition of a surplus amount of pure drug and optimized nanosuspension in 10 mL of distilled water. Then, samples were agitated using an orbital shaker (Remi instruments limited, Mumbai) for 48 h at 25°C, then centrifuged to remove the solid content as a residue and the amount of drug present in the supernatant layer was analyzed spectrophotometrically using a UV-visible spectrophotometer at 260 nm.

### Total drug content (TDC)

An aliquot of nanosuspension (0.5 mL) was dried by evaporation. Further the residue was dissolved in methanol followed by filtration using 0.45  $\mu$ m filter paper. The samples were then analyzed using a UV-visible spectrophotometer (Shimadzu-1700, Japan) at  $\lambda$  max of 260 nm. The TDC and percentage TDC were calculated from equations 1 and 2.

**Table 1:** CCD matrix with predicted and observed values of responses

Independent variables				Dependent variables					
Batch	A (mg)	B (mg)	C	Observed values			Predicted values		
				Y1* (nm)	Y2* (%)	Y3* (%)	Y1 (nm)	Y2 (%)	Y3 (%)
1	0	0	-1.68179	225.00	91.26	99.71	233.17	91.27	98.73
2	0	0	0	215.00	87.75	99.66	219.93	87.56	99.25
3	0	0	0	204.00	87.23	99.67	219.93	87.56	99.25
4	-1	1	1	220.00	93.69	99.99	235.38	94.03	99.61
5	0	0	0	225.00	87.84	99.66	219.93	87.56	99.25
6	1	-1	1	192.00	86.23	98.59	217.90	87.43	98.66
7	0	0	1.68179	228.00	89.80	99.76	222.35	89.55	99.77
8	1.68179	0	0	302.00	92.57	99.44	280.83	92.45	99.11
9	0	-1.68179	0	229.00	89.32	99.73	240.18	88.19	98.80
10	-1.68179	0	0	225.00	90.89	99.57	248.69	90.77	99.39
11	-1	-1	-1	235.00	90.61	98.26	236.23	91.69	98.69
12	1	-1	-1	278.00	95.46	96.67	260.84	95.29	98.28
13	-1	1	-1	233.00	89.24	97.61	205.32	88.21	98.75
14	0	0	0	226.00	87.02	99.67	219.93	87.56	99.25
15	1	1	-1	265.00	88.40	99.95	293.43	88.64	100.04
16	0	0	0	228.00	87.96	99.67	219.93	87.56	99.25
17	0	0	0	222.00	87.50	99.67	219.93	87.56	99.25
18	0	1.68179	0	249.00	88.56	99.70	240.34	89.46	99.70
19	1	1	1	252.00	93.34	98.88	248.99	92.42	99.68
20	-1	-1	1	298.00	85.94	99.16	267.79	85.87	100.29

\*Y1: Particle size; \*Y2: Drug content; \*Y3: Entrapment efficiency, CCD: Central composite design

$$\text{TDC} = (\text{Vol. total}/\text{Vol. aliquot}) \times \text{drug in aliquot} \times 100 \quad (1)$$

$$\% \text{TDC} = \text{TDC}/\text{TAD} \times 100 \quad (2)$$

Where vol. total/vol. aliquot is the total volume of nanosuspension.

The total amount of drug, that is, TAD is the drug used for the preparation of nanosuspension.

### Entrapment efficiency

Entrapment efficiency (%EE) was determined using ultracentrifugation of 2 mL of sample for 30 min at 10,000 rpm at 4°C using a cold centrifuge (Remi CM 12 Plus, Mumbai). The supernatant was used to determine free drug content (FDC). Obtained sediment was washed with a 0.1 N NaOH solution to determine surface adsorbed drugs (SAD). Using a UV-visible spectrophotometer, all drug solutions were quantified in triplicates at 260 nm. PC is the percentage of drug entrapped in nanoparticles and can be calculated using the given formula,<sup>[10]</sup>

$$\% \text{EE} = \text{TDC} - (\text{FDC} + \text{SAD})/\text{TAD} \times 100.$$

### Determination of particle size and zeta potential (ZP)

The size and ZP of optimized nanosuspension were measured using Zetasizer 300 HAS (Malvern Instruments, Malvern, UK). Before size determination, optimized nanosuspension was dispersed in distilled water. Data obtained were mean average values of three independent samples that are prepared under the same formulation conditions.<sup>[11]</sup>

### Differential scanning calorimetry (DSC)

The thermal behavior of pure drug, physical mixture (PM) with excipients, and optimized nanosuspension were studied using a Perkin Elmer 4000e module controlled by PYRIS Version – 11.1.0.0488 (PerkinElmer, Inc., USA.). For each analysis, before heating under nitrogen purging (20 mL/min), the samples of 1 mg were kept in sealed aluminium pans and scanned at a scanning rate of 10°C/min for a temperature range of 3°C–350°C.

### Fourier-transform infrared spectroscopy (FTIR)

FTIR of a drug, PM, and optimized nanosuspension was analyzed using the FTIR spectrophotometer (Agilent CARY

630 FTIR) to study the compatibility between drug and stabilizers. Every specimen was analyzed by keeping them on ATR diamond crystal by pro software of Agilent Resolutions. Every spectrum of samples was collected from an average of 21 single scans at  $4\text{ cm}^{-1}$  resolution in the absorption area of  $800\text{--}4000\text{ cm}^{-1}$ .<sup>[12]</sup>

## Solid-state characterization

### Scanning electron microscope (SEM)

The SEM was used to study the morphology of the surface of posaconazole nanosuspensions which examine the surface properties of nanosuspension. SEM studies were done using SEM (JEOL JSM-6360, Japan) at 20 kV accelerating voltage and high vacuum. Before analysis, optimized nanosuspension was first placed on two-sided carbon tape and, then, sputtered with gold-palladium alloy up to 3–5 nm of thickness.<sup>[13]</sup>

### Powder X-ray diffractometry (XRD)

The XRPD spectra of pure drug, PM, and optimized nanosuspension were obtained using an X-ray diffractometer (Philips analytical XRD, PW 3710) with Cu-K $\alpha$  radiation (1.54 Å), at 40 kV, 40 mA by passing through a nickel filter. The samples were analyzed in the  $2\theta$  angle range of  $5\text{--}80^\circ$ . The range and the chart speed were  $5 \times 10^3$  CPS and  $10\text{ mm}/^\circ 2\theta$ , respectively.<sup>[14]</sup>

### In vitro drug release studies

Dissolution studies on pure drug and their optimized nanosuspension were performed using USP type-II apparatus. Weighed quantities of samples were transferred into the dissolution apparatus (Electro lab TDT-08 L, India) containing 900 mL of SGF with pH 1.2, simulated intestinal fluid with pH 6.8 and pH 7.4, respectively, as a medium. The shaft speed was set to 50 rpm at a medium temperature of  $37 \pm 0.5^\circ\text{C}$ . Samples (5 mL each) were withdrawn at 10, 20, 30, 40, 50, and 60 min of time points and the fresh buffer was added for sink condition maintenance. The samples were collected and filtered using the Whatman filter paper (0.25  $\mu\text{m}$ , Whatman Inc., USA) and inspected using a UV spectrophotometer at 260 nm.<sup>[15-25]</sup> The release profile of nanosuspension was correlated with the pure drug.

### Pharmacokinetic (PK) study

Adult male albino Wistar rats weighing 200–250 g (4–8 weeks) were used for the study. They were housed in polypropylene cages and were maintained at a room temperature of  $23^\circ\text{C} \pm 2$  and a relative humidity 50%. They were maintained in 12 h: 12 h light: dark cycle throughout the period of acclimatization and experimental study. Animals were provided with a standard rodent pellet diet. Food and water were allowed *ad libitum*. All Wistar rats were fed a normal laboratory chew diet (Nutrilab Rodent

Fed, PROVIMI) containing (W/W) of 21.88% crude proteins, 52.15% carbohydrates, and 5.97% crude fat. The experiments were planned after the approval of the Institutional Animal Ethical Committee (IAEC).<sup>[15]</sup> The proposed protocol of the posaconazole nanosuspension in healthy Wistar rats accepted by the Animal Ethical committee of Pulla Reddy Institute of Pharmacy, Hyderabad with CPCSEA No: IAEC-II-PRIP-NOV-2021-PROTOCOL-1, Dated: November 15, 2021.

## Procedure

Each group contains six rats that they were fasted for 24 h before the experiments and given free access to the water. Pure drug posaconazole (10 mg/kg is suspended in 0.5% methylcellulose prepared in water for injection) and optimized nanosuspension at a dose equivalent to 10 mg/kg of posaconazole were administered orally. Blood samples (1 mL) were collected at time points of 0.5, 1, 2, 4, 8, 12, and 24 h post-dose and transferred to ethylene diamine tetra acetic acid (EDTA)-coated tubes to prevent coagulation. Then, blood samples were centrifuged at 5000 rpm for 10 min and the obtained plasma samples were stored at  $-10^\circ\text{C}$  until analysis.

### HPLC analysis

Rats plasma sample's concentration of posaconazole was estimated using HPLC Method (USP Method) with Minor Modifications. Waters HPLC (2695 Separation Module), with PDA Detector, and Zorbax SB ODS C<sub>18</sub> Column (150 Mm  $\times$  4.6 Mm, 5  $\mu\text{m}$ ) are used for the estimation. Reverse phase chromatography was utilized for estimation of posaconazole. The column and instrument temperature was maintained at room temperature. Mobile phase was buffer:acetonitrile (40:60 v/v), with a flow rate of 1 ml/min, volume of injection is 20  $\mu\text{L}$ . The detection wavelength was 260 nm and temperature was maintained at  $25^\circ\text{C} \pm 2^\circ\text{C}$ .

### Statistical analysis

The PK parameters, such as  $C_{\text{max}}$ ,  $t_{\text{max}}$ ,  $\text{AUC}_{\text{total}}$ ,  $t_{1/2}$ , and mean residence time (MRT), were calculated using Kinetica software (version 5.0). One-way ANOVA was used for the statistical analysis of three groups by GraphPad prism software (version 2017).

### Stability studies

The stability studies were performed as per ICH Q1A (R2) guidelines for the optimized nanosuspension. The formulations were placed in HDPE bottles and stored at three temperature conditions:  $4^\circ\text{C}$  (refrigerator), room temperature and  $40^\circ \pm 2^\circ\text{C}/75 \pm 5\% \text{ RH}$  (stability Chamber) for 6 months and further evaluated for drug content, particle size, and % CDR to study the physicochemical stability of product.<sup>[16]</sup>

## RESULTS AND DISCUSSION

### Optimization of experimental design

By design of expert, 20 runs were proposed and the input of predicted and observed values for particle size (Y1), drug content (Y2), and entrapment efficiency (Y3) responses ranges from 192 to 302 nm, 86.23 to 95.46%, and 99.16 to 99.99%, respectively. With the help of design expert software, the obtained responses simultaneously fitted to cubic, 2FI, quadratic, and linear models. As the  $R^2$  value was found  $>0.9$  and both values of the predicted and observed were less comparable with standard deviations (SD) ( $<1.0\%$ ) and values of precision; thus, the best-fitted model for Y1 and Y2 was quadratic and 2FI for Y3.

### Effect on size of particle (Y1)

The proposed polynomial equation for particle size is as follows,

$$Y1 = +219.93 + 9.56(A) + 0.0466(B) - 3.22(C)$$

Where, Y1 is particle size, (A) concentration of tween 80, (B) concentration of soya lecithin, and (C) the number of cycles for optimized nanosuspension formulation by high-pressure homogenization.

The models were significant as the F value was  $<0.002$ , while model terms obtained were significant as the Prob  $>F$   $P < 0.0500$ ; hence, these models are used to develop the design space. In this case, AC and  $A^2$  are the two model terms used for design space.

The impact of independent factors on particle size (Y1) was studied using 3D response surface plots. The Y1 responses predicted values range from 205.32 to 293.42 nm. The positive value of the coefficient represents an increasing Y1. According to the findings depicted in Figure 1, particle aggregates as tween 80 concentration (A) rise from 0.10 to 0.30 mg. Surfactant saturation in nanosuspension causes produced particles to be absorbed by an excess surfactant

concentration. When soya lecithin (B) concentration rises from 10 to 30 mg, it no longer prevents the re-aggregation of dispersed particles, resulting in the presence of bigger bodies in the nanosuspension and increasing particle size. Hence, the increased concentration of surfactant and polymer increases the particle size. The number of cycles (C) for HPH shows a direct relationship with particle size, with a rise in number of cycles of HPH showing a decrease in the particle size. The coefficient with negative value represents decreasing particle size. An increase in the number of cycles leads to a reduction in the size of the particle by increasing the viscosity of the system, which inhibits the Ostwald ripening. Hence, the increase in number of cycles leads to a rise in the dynamic pressure with a decreased static pressure at room temperature, below the water boiling point.

### Effect on drug content (Y2)

The proposed polynomial equation for drug content is as follows,  $Y2 = +87.56 + 0.4972(A) + 0.3770(B) - 0.5099(C)$ .

The predicted Y2 response values range from 85.87 to 95.29%. The models were significant as the F value was  $<0.0001$ , while model terms were significant as the Prob  $>F$   $P < 0.0500$ ; hence, these models AC and BC are used to develop the design space. An increase in the amount of "Tween 80 (A)" leads to an increase in drug content, while the concentration of SL "B" shows a negligible effect on drug content [Figure 2]. The drug content decreases with increasing number of cycles ("C"). The quantity of the drug, that is, dose present in nanoparticles is significant to study dissolution and PK parameters. However, drug content has the most significant effect on drug dissolution, which directly affects drug absorption and therefore bioavailability.

### Effect on entrapment efficiency (Y3)

The proposed polynomial equation for entrapment efficiency is as follows,

$$Y3 = +99.25 - 0.0848(A) + 0.2693(B) + 0.3085(C)$$

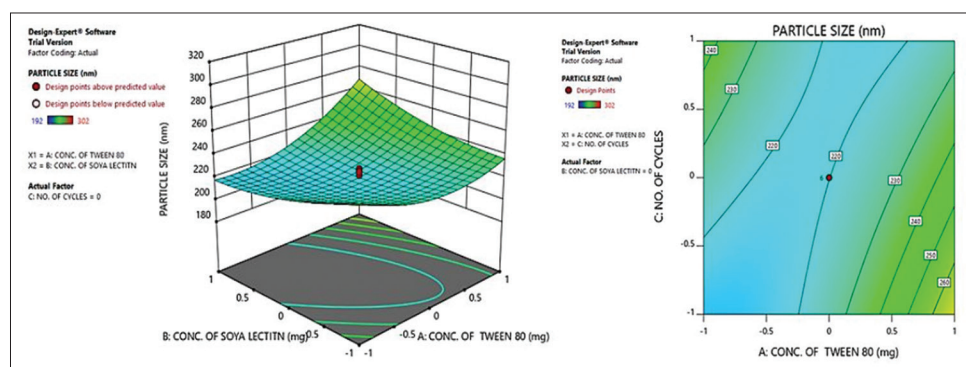
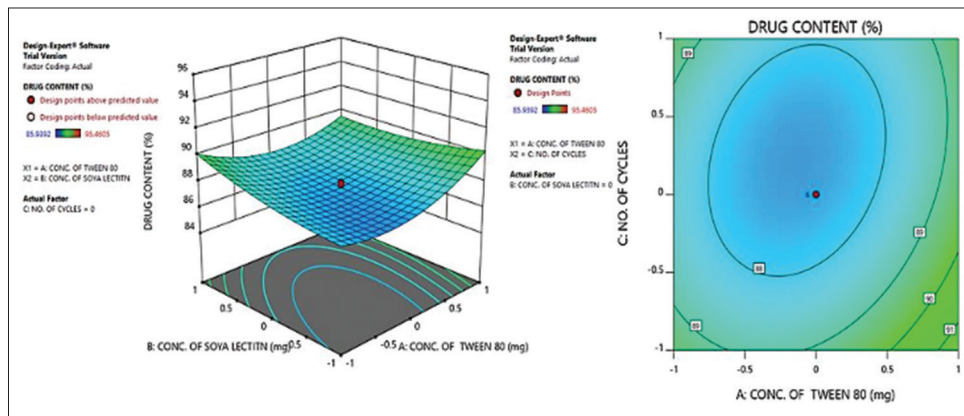
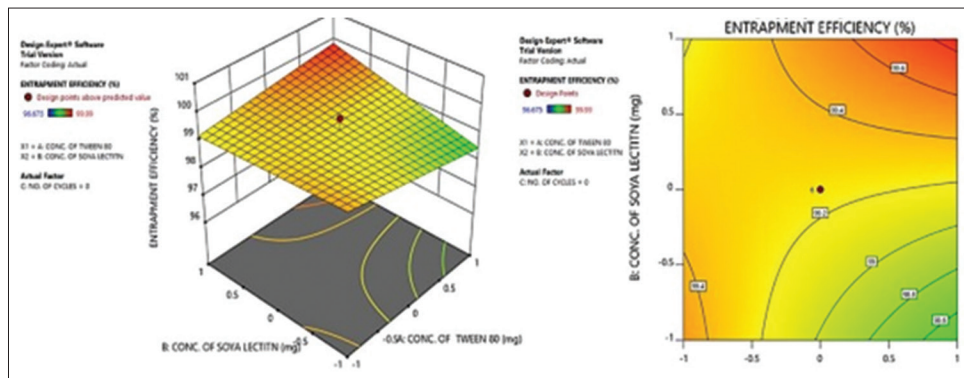


Figure 1: Contour plot and response surface plots of particle size



**Figure 2:** Contour plot and response surface plots of drug content



**Figure 3:** Contour plot and response surface plots of entrapment efficiency

The predicted values of Y3 are reported in Table 1 and range from 96.675 to 99.99%. The models were significant as the F value was  $<0.0001$ . Here, in this model, conc of soya lecithin (B) and number of cycles (C) terms are significant. The 3D surface plot of response is displayed in Figure 3 which predicts that the % entrapment efficiency increases with increased values of conc of soya lecithin (B) and number of cycles (C). Due to the significant interaction of soya lecithin in nanosuspensions, optimum entrapment efficiencies control the release of drugs from nanosuspensions. Entrapment efficiency increases the drug loading capacity of nanosuspensions with increased dosing intervals. Thus, it is a CQA and the factors, that is, concentration of soya lecithin and a number of homogenization cycles, which affect entrapment efficiency, were optimized by CCD.

## DSC

The results of the DSC analysis are displayed in Figure 4. Coarse posaconazole powder showed a distinct endothermic peak at  $184.41^{\circ}\text{C}$ , which was the marked intrinsic melting point peak of PC, while DSC of the PM showed two distinct melting endotherms at  $166.85^{\circ}\text{C}$  and  $178.63^{\circ}\text{C}$ . In addition, mannitol showed a sharp endothermic peak at  $168.74^{\circ}\text{C}$ , which indicates its high crystallinity. The mixture of drug and excipients demonstrated an exothermic peak at  $164.34^{\circ}\text{C}$ ; thus, it was inferred that the final combination mixture

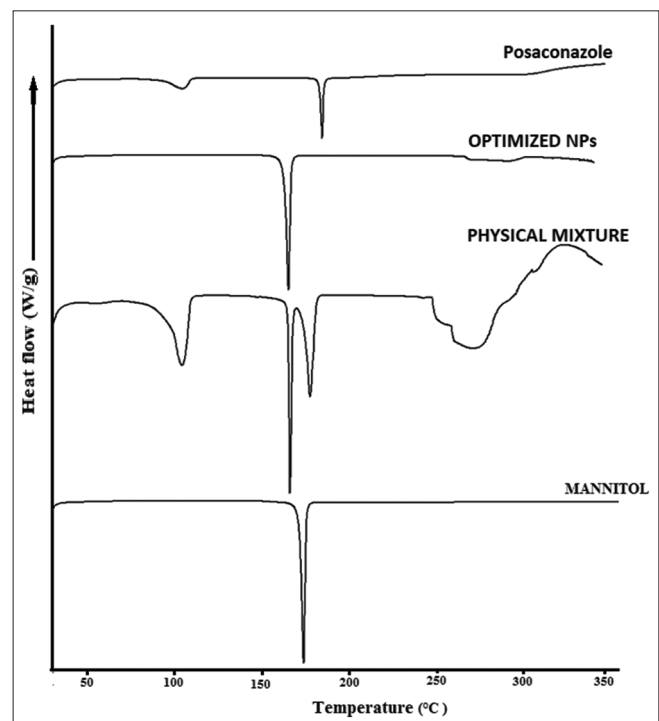


**Figure 4:** DSC analysis of posaconazole, optimized nanosuspension, physical mixture, and mannitol

remains in its normal form and has not undergone any interaction with excipients proposed within the formulation.

## FTIR

The FTIR spectra of the drug, PM, and nanosuspension are disclosed in Figure 5. The FTIR spectra of the drug revealed the characteristic peaks at 3369.546 and 3288.872  $\text{cm}^{-1}$  relate to intermolecular polymeric OH bonding, while 2974.151  $\text{cm}^{-1}$  peak indicates C-H stretching of  $\text{CH}_3\text{-CO}$  group, 2921.704 and 2853.140  $\text{cm}^{-1}$  revealed C-H stretching of  $>\text{CH}_2$  group, while 1584.659  $\text{cm}^{-1}$  is attributed to acids, that is, C=O stretching. The characteristic peak at 1356.175  $\text{cm}^{-1}$ , 1283.928  $\text{cm}^{-1}$ , and 1058.227 attributed to C-H deformation of  $-\text{CH}_2\text{-CO-}$  group, C-O stretching, and O-H deformation (in-plane) of a secondary alcohol, and C-O stretching of alkyl, respectively. Intense peaks were also found at 912  $\text{cm}^{-1}$ , 818.348  $\text{cm}^{-1}$ , 785.975  $\text{cm}^{-1}$ , and 679.119  $\text{cm}^{-1}$  which are attributed to C-H deformation as aldehydes, =C-H stretching and deformation of alkenes  $\text{R}_1\text{R}_2\text{C}=\text{CHR}_3$ , C-H out-of-plane deformation of three adjacent hydrogen atoms,

and =C-H stretching and deformation of  $\text{CH}=\text{CH}$  (cis), respectively [Figure 5]. The FTIR spectra of nanosuspension show a broadening of peaks at 3269.073  $\text{cm}^{-1}$  of OH bonding and C-H stretching at 2935.012  $\text{cm}^{-1}$  which may be due to the diluting effect of mannitol or maybe due to the formation of the hydrogen bond between the N-H groups of soya lecithin with the carbonyl group of the drug. All the characteristic peaks of the drug are available in the PM indicating compatibility between the drug and excipients, which confirms that there was no chemical modification of the drug and the chemistry of the drug remains as such.

## SEM

Posaconazole is a coarse micronized powder with a fine white texture and has poor aqueous solubility. The coarse PC particles bear an average size of particle 5–7  $\mu\text{m}$  with broad size distribution observed in SEM. The SEM of

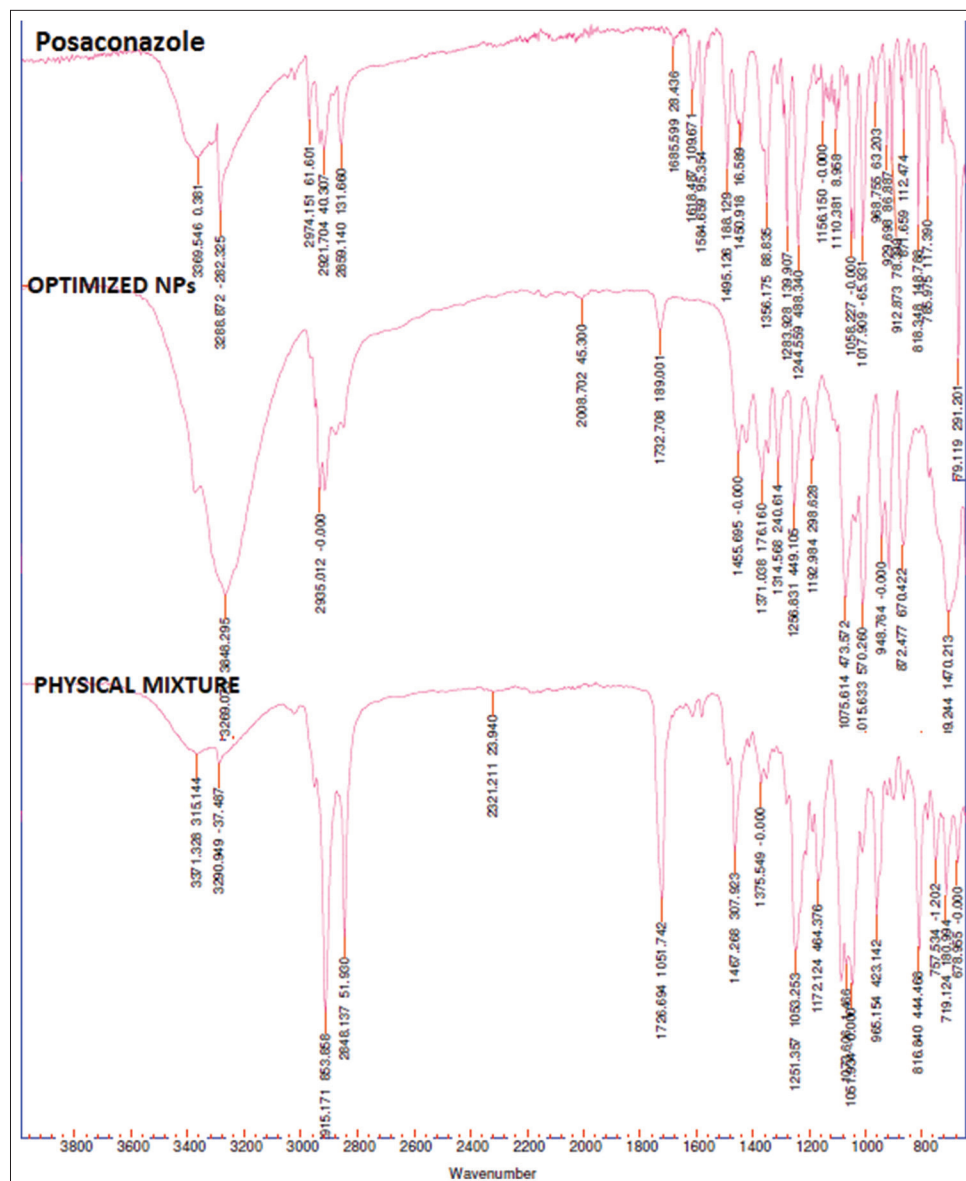


Figure 5: FTIR analysis of posaconazole, optimized nanosuspension, and physical mixture

optimized lyophilized nanosuspensions showed that particles were discrete with an absence of agglomeration due to the presence of a stabilizer. They had porous surfaces and were slightly elongated and needle in shape but not completely spherical in shape. SEM images of nanosuspensions showed quasi-spherical spheres [Figure 6].

### Powder XRD (PXRD)

The XRPD patterns of powder drug, PM, and optimized nanosuspension are displayed in Figure 7. Five sharp characteristic diffraction peaks were exhibited by the drug at  $2\theta$  of  $13.54^\circ$ ,  $15.36^\circ$ ,  $16.5^\circ$ ,  $18.0^\circ$ , and  $19.42^\circ$  and several short peaks were between  $2\theta$  of  $10.66^\circ$  and  $32.36^\circ$ , indicating its high crystalline nature. The PM demonstrated two reflections at  $2\theta$  of  $20.52^\circ$  and  $21.66^\circ$  with the lowest intensities compared to drug and nanosuspensions. Nanosuspensions showed six diffraction lines but at lesser intensities as compared to a drug at  $2\theta$  of  $9.5^\circ$ ,  $10.76^\circ$ ,  $13.52^\circ$ ,  $17.14^\circ$ ,  $19.86^\circ$ ,  $20.28^\circ$ ,  $21.2^\circ$ ,  $27.4^\circ$ ,  $30.28^\circ$ , and  $31.42^\circ$  with the additional peaks of mannitol [Figure 7].

### In vitro drug release studies

The dissolution behavior of the pure drug posaconazole along with the optimized nanosuspension in different

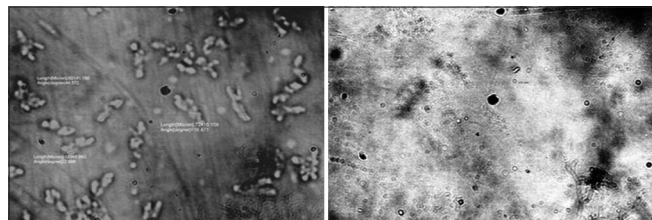


**Figure 6:** SEM images of posaconazole nanosuspension

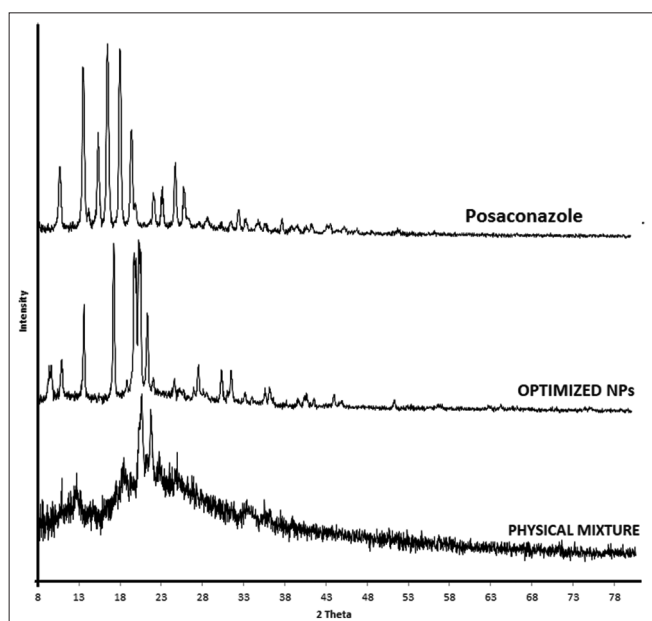


**Figure 7:** XRD analysis of posaconazole, optimized nanosuspension, and physical mixture

pH is represented in Figure 8. The release of pure drug and optimized nanosuspension was found to be  $25.375 \pm 0.063\%$  and  $96.313 \pm 0.054\%$  within 60 min in SIF pH 6.8, respectively, while SIF pH 7.4 – showed  $20.533 \pm 0.011\%$  and  $97.883 \pm 0.060\%$  release and SGF pH 1.2 – showed  $26.199 \pm 0.04\%$  and  $95.101 \pm 0.025\%$  release, respectively. The rate of dissolution of optimized nanosuspension enhanced significantly as compared to the posaconazole drug by 4.76 folds in pH SIF 7.4. The optimized nanosuspension displayed a significant increase in dissolution profile, by more than 4 folds on average as compared to the drug within 60 min. The dissolution profile of optimized nanosuspension was higher in SIF pH 7.4, followed by SIF pH 6.8 and SGF pH 1.2. This indicates dissolution profile of the optimized nanosuspension was distinctly superior as compared to the drug.

### PK studies

The PK parameters such as maximum concentration of serum ( $C_{max}$ ), time to reach the maximum concentration of serum ( $T_{max}$ ), area obtained under the plasma concentration-time curve (AUMC), MRT, and clearance ( $Cl_r$ ) prove the bioavailability of formulation. The results are shown in Table 2.

$C_{max}$  of posaconazole market and nanosuspension were  $0.885 \pm 0.5 \mu\text{g/mL}$  and  $2.320 \pm 0.06 \mu\text{g/mL}$ , respectively, with significantly no difference ( $P < 0.05$ ).  $T_{max}$  values of the posaconazole market and optimized nanosuspension were  $0.52 \pm 0.25 \text{ h}$  and  $1.087 \pm 0.25 \text{ h}$ , respectively, with significant variance ( $P < 0.05$ ) and  $P < 0.0005$ . Due to the subjective variability, there was variance in individual  $T_{max}$  and  $C_{max}$  values. The results of PK parameter values designate that the marketed formulation and optimized nanosuspension were completely different since the produced formulation releases the medicine for the longest possible time with the greatest bioavailability.

### Stability studies

The 6-month stability data for optimized nanosuspension stored at refrigerated temperature showed insignificant increase in particle size from  $199.2 \pm 6.98 \text{ nm}$  to  $221.6 \pm 3.8 \text{ nm}$ , while storage under room temperature conditions showed a slight increase from  $199.2 \pm 6.98 \text{ nm}$  to  $240.9 \pm 4.01 \text{ nm}$ , respectively. The nanosuspension stored at  $40^\circ \pm 2^\circ\text{C}$  showed an increase in the size of particles from  $199.2 \pm 6.98 \text{ nm}$  and  $275.6 \pm 5.2 \text{ nm}$ , respectively.

Nanosuspension at the refrigerator conditions shows better stability as compared to room temperature and  $40^\circ\text{C}$  (ACC) conditions which may be attributed to the aggregation of nanoparticles with a rise in temperature [Table 3]. Figure 9 shows the particle size variation with respect to time (2,4 and 6months).



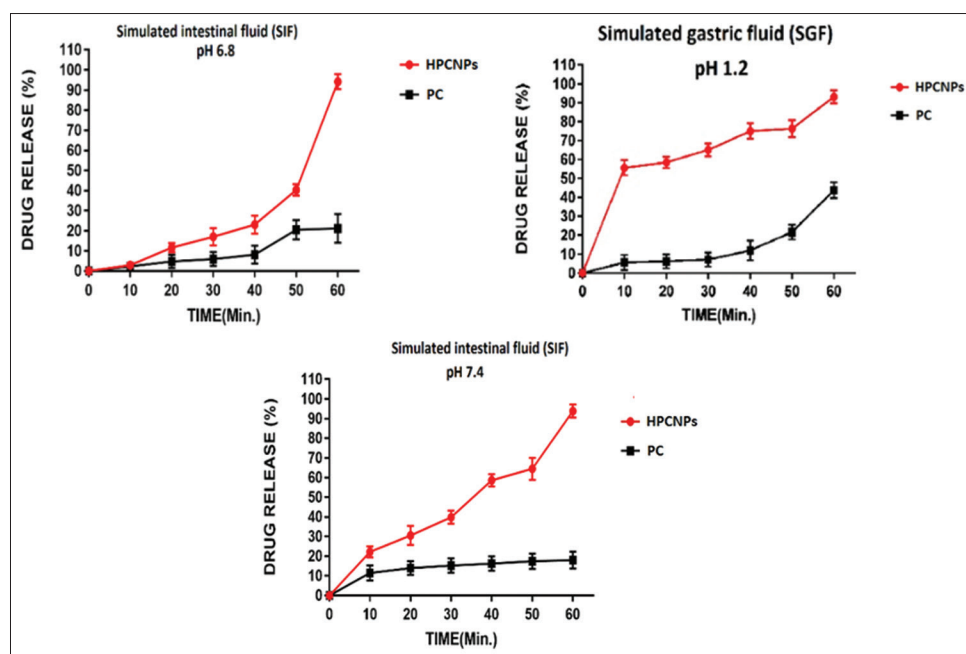
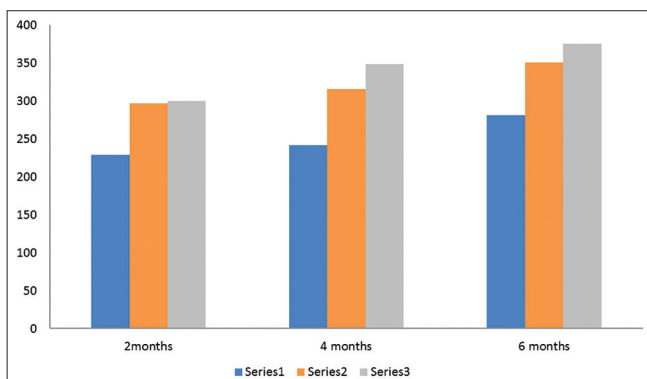
**Table 2:** Comparative bioavailability parameters of reference and test formulations

PK parameter	Marketed suspension	Nano-suspension	"t"-test at 0.05
C <sub>max</sub> (µg/mL)	0.885	2.320	Significant
T <sub>max</sub> (h)	0.522	1.087	Significant
MRT (h)	0.078	0.148	Significant
Total AUMC (µg-h/mL)	332.54	856.22	Significant
Cl (mL/min)	124.81	181.63	Significant

MRT: Mean residence time

**Table 3:** Physical stability data of optimized nanosuspension for the 6-month stability study

Formulation	Storage temperature conditions	Initial particle size	Particle size (nm)		
			2 months	4 months	6 months
Nanosuspensions	4°C	199.2±6.98	209.1±2.3	211.6±3.3	221.6±3.8
	Room temperature		216.8±4.2	225.8±4.6	240.9±4.0
	40°C		220.2±2.9	248.9±2.6	275.6±5.2

**Figure 8:** Drug release analysis of optimized nanosuspension (HPCNPs) and pure drug (PC) in simulated intestinal fluid (SIF) with pH 6.8, simulated intestinal fluid (SIF) pH 7.4, simulated gastric fluid (SGF) with pH 1.2**Figure 9:** The particle size variation with respect to time (months)

## CONCLUSION

Posaconazole formulated nanosuspension was optimized using CCD. The morphology studies (PXRD and SEM) showed the amorphous state of the drug. *In vitro* drug release of nanosuspension was higher than that of pure drugs. Formulating the drug into nanosuspension shows improvements in oral bioavailability when compared with the marketed formulation. The stability studies indicate that the formulation was stable for up to 6 months. The QbD approach was used to study the impact of CPPs and CMAs on CQAs, which helps to improve the safety and quality of the formulation. The critical material attributes such as conc of Tween 80, conc of soya lecithin, and process parameters such

as number cycles of homogenization were screened using the method PB. The CCD of RSM was used for the optimization of the nanosuspension.

Further, evaluation of the optimized nanosuspension was performed. The results obtained have proved that the HPH technique was better for the formulation of uniform particle size and also for stabilizing the nanoparticles. Furthermore, with QbD concept implementation, very fewer runs of experiments are used for the optimization of nanosuspension, which is the evidence for the reduction in the manufacturing cost, while the least values of residual error obtained are the evidence for reduction of manufacturing variability. The intended characteristics of nanosuspension are confirmed by the small particle size, lowest PDI values, increased drug content, smooth and spherical particles with higher entrapment efficiency, and improved bioavailability. Based on the results, it is inferred that the QbD is an effective tool in novel drug delivery systems, which is a key demand of the USFDA and for the India Market to decrease production variability, increase safety and quality, and lower manufacturing costs.

## ACKNOWLEDGMENT

The authors are very thankful to Parul University, Vadodara, Gujarat for continuous support and guidance during this research work and special thanks to Pulla Reddy institute of Pharmacy, Hyderabad, Telangana for providing the facilities to carry out research work.

## REFERENCES

- Pouton CW. Lipid formulations for oral administration of drugs: Non-emulsifying, self-emulsifying and “self-microemulsifying” drug delivery systems. *Eur J Pharm Sci* 2000;11:93-8.
- Hauss DJ. Oral lipid-based formulations. *Adv Drug Deliv Rev* 2007;59:667-76.
- Yang M, Dong Z, Zhang Y, Zhang F, Wang Y, Zhao Z. Preparation and evaluation of posaconazole-loaded enteric microparticles in rats. *Drug Dev Ind Pharm* 2017;43:618-27.
- Patel R, Shah D. Nanoparticles loaded sublingual film as an effective treatment of chemotherapy-induced nausea and vomiting. *Int J PharmTech Res* 2015;8:77-87.
- Hwang RC, Kowalski DL. Design of experiments for formulation development. *Pharm Technol* 2005;7:1-5.
- Singh B, Kumar R, Ahuja N. Optimizing drug delivery systems using systematic “design of experiments.” Part I: Fundamental aspects. *Crit Rev Ther Drug Carrier Syst* 2005;22:97-105.
- Gonzalez-Mira E, Egea M, Souto EB, Calpena AC, García ML. Optimizing flurbiprofen-loaded NLC by central composite factorial design for ocular delivery. *Nanotechnology* 2011;22:045101.
- Jacobs C, Kayser O, Muller RH. Production and characterization of mucoadhesive nanosuspensions for the formulation of bupravaquone. *Int J Pharm* 2001;214:3-7.
- Madhav KV, Kishan V. Improvement of anti-hyperlipidemic activity and oral bioavailability of fluvastatin via solid self-microemulsifying systems and comparative with liquisolid formulation. *Curr Drug Deliv* 2018;15:1245-60.
- Moschwitz J, Achleitner G, Pomper H, Muller RH. Development of an intravenously injectable chemically stable aqueous omeprazole formulation using nanosuspension technology. *Eur J Pharm Biopharm* 2004;58:615-9.
- Katla VM, Veerabrahma K. Cationic solid self micro emulsifying drug delivery system (SSMED) of losartan: Formulation development, characterization and *in vivo* evaluation. *J Drug Deliv Sci Technol* 2016;35:160-9.
- Rakesh P, Charmi P. Quantitative analytical applications of FTIR spectroscopy in pharmaceutical and allied areas. *J Adv Pharm Educ Res* 2014;4:145-57.
- Kumar VV, Chandrasekhar D, Ramakrishna S, Kishan V, Rao YM, Diwan PV. Development and evaluation of nitrendipine loaded solid lipid nanoparticles: Influence of wax and glyceride lipids on plasma pharmacokinetics. *Int J Pharm* 2007;335:167-75.
- Dudhipala N, Veerabrahma K. Improved anti-hyperlipidemic activity of rosuvastatin calcium via lipid nanoparticles: Pharmacokinetic and pharmacodynamic evaluation. *Eur J Pharm Biopharm* 2017;110:47-57.
- Kim DW, Kwon MS, Yousaf AM, Balakrishnan P, Choia HG. Comparison of a solid SMEDDS and solid dispersion for enhanced stability and bioavailability of clopidogrel napadisilate. *Carbohydr Polym* 2014;114:365-74.
- Madhav KV, De S, Shekar C, Babu GS. Fenofibrate solid dispersion for improving oral bioavailability: Preparation, characterization and *in vivo* evaluation. *Int J Pharm Sci Nanotechnol* 2021;13:5102-9.
- Trotta M, Gallarate M, Patarino F, Morel S. Emulsions containing partially water-miscible solvents for the preparation of drug nanosuspensions. *J Control Release* 2001;76:119-28.
- Byrne JD, Betancourt T, Brannon-Peppas L. Active targeting schemes for nanoparticle systems in cancer therapeutics. *Adv Drug Deliv Rev* 2008;60:1615-26.
- Yoncheva K, Lizarraga E, Irache JM. Pegylated nanoparticles based on poly(methyl vinyl ether-co-maleic anhydride): Preparation and evaluation of their bioadhesive properties. *Eur J Pharm Sci* 2005;24:411-9.
- Isabela PV, Daniel JS, Eduardo CC, Garcia JS, Trevisan MG. Development, characterization, and stability studies of ethinyl estradiol solid dispersion. *J Therm Anal Calorim* 2015;120:573-81.
- Kayaert P, Li B, Jimidar I, Rombaut P, Ahssini F, Van den Mooter G. Solution calorimetry as an alternative approach for dissolution testing of nanosuspensions. *Eur J Pharm Biopharm* 2010;76:507-13.

22. Kayaert P, Van den Mooter G. An investigation of the adsorption of hydroxypropylmethyl cellulose 2910 5 mPa s and polyvinylpyrrolidone K90 around Naproxen nanocrystals. *J Pharm Sci* 2012;101:3916-23.
23. Lalitha Y, Lakshmi PK. Enhancement of dissolution of nifedipine by surface solid dispersion Technique. *Int J Pharm Sci* 2011;3:41-6.
24. Langguth P, Hanafy A, Frenzel D, Grenier P, Nhamias A, Ohlig T, *et al.* Nanosuspension formulations for low-soluble drugs: Pharmacokinetic evaluation using spironolactone as model compound. *Drug Dev Ind Pharm* 2005;31:319-29.
25. Liang L, Lin SW, Dai W, Lu JK, Yang TY, Xiang Y, *et al.* Novel cathepsin B-sensitive paclitaxel conjugate: Higher water solubility, better efficacy and lower toxicity. *J Control Release* 2012;160:618-29.

**Source of Support:** Nil. **Conflicts of Interest:** None declared.